archives
of thermodynamics
Vol. **37**(2016), No. 3, 45–62
DOI: 10.1515/aoter-2016-0019

Parametric study of fluid flow and heat transfer over louvered fins of air heat pump evaporator

TOMASZ MUSZYŃSKI[a]
SŁAWOMIR MARCIN KOZIEŁ[a,b*]

[a] Gdansk University of Technology, Narutowicza 11/12, 80-233 Gdańsk, Poland

[b] Reykjavik University, Menntavegur 1, 101 Reykjavik, Iceland

Abstract Two-dimensional numerical investigations of the fluid flow and heat transfer have been carried out for the laminar flow of the louvered fin-plate heat exchanger, designed to work as an air-source heat pump evaporator. The transferred heat and the pressure drop predicted by simulation have been compared with the corresponding experimental data taken from the literature. Two dimensional analyses of the louvered fins with varying geometry have been conducted. Simulations have been performed for different geometries with varying louver pitch, louver angle and different louver blade number. Constant inlet air temperature and varying velocity ranging from 2 to 8 m/s was assumed in the numerical experiments. The air-side performance is evaluated by calculating the temperature and the pressure drop ratio. Efficiency curves are obtained that can be used to select optimum louver geometry for the selected inlet parameters. A total of 363 different cases of various fin geometry for 7 different air velocities were investigated. The maximum heat transfer improvement interpreted in terms of the maximum efficiency has been obtained for the louver angle of 16 ° and the louver pitch of 1.35 mm. The presented results indicate that varying louver geometry might be a convenient way of enhancing performance of heat exchangers.

Keywords: Heat exchangers; Heat transfer intensification; CFD, Convection; Air source heat pump

*Corresponding Author. E-mail: koziel@ru.is

Nomenclature

c	–	specific heat, W/kg K
Fp	–	fin pitch, m
Ft	–	fin thickness, m
h	–	heat transfer coefficient, W/m^{2}K
H	–	louver width, m
k	–	conductivity, W/m K
Lp	–	louver pitch, m
ΔP	–	pressure drop, Pa
$\dot{\mathrm{Q}}$	–	heat flux, W
T	–	temperature, °C or K
ΔT	–	temperature drop, K
u, v, w	–	velocity components, m/s
$\dot{\mathrm{V}}$	–	volumetric flow rate, m^3/s
x, y, z	–	Cartesian coordinates

Greek symbols

α	–	louvers angle, deg
ρ	–	density, kg/m^3
η	–	thermal performance index

Subscripts

air	–	air
h	–	hydraulic
i, k	–	vectot components
in	–	inlet
out	–	outlet
p	–	at constant pressure,

1 Introduction

Heat exchangers play an important role in almost every engineering system [1]. Their primary purpose is heat transfer between two working fluids such as air, refrigerants, water, glycols, etc. For example, air-to-refrigerant exchangers are used in refrigeration and air conditioning [2], automotive [3], as well as heat pump industry [4]. One of the most important design challenges for this type of devices is improvement of their efficiency, especially the heat transfer rate [5,6]. In compact heat exchangers, thermal resistance is generally dominant on the air side and may account for over 80% of the total thermal resistance. The air-side heat transfer surface area is up to 10 times larger than the water-side one. However, water-side heat transfer coefficient is approximately 50 times higher than air-side one. Thus, the air-side thermal resistance turns out to be higher by a factor of five. Con-

sequently, any improvement in the heat transfer on the air side improves the overall performance of the heat exchanger. Louvered fins are frequently used on the air side of air conditioning evaporators and other heat exchangers to enhance the overall heat transfer rate. The louvers act to interrupt the air flow and create a series of thin boundary layers which have lower thermal resistance than the thick boundary layers on the plain fins [7]. Optimization of heat exchanger geometry may considerably improve energy savings in these systems [8]. On the other hand, improved efficiency leads to reduced exchanger size, thus significantly reduces its manufacturing cost, and annual energy expenditures related to pumping [9].

Unfortunately, optimization and design improvement of heat exchangers is a very challenging task. Experimental studies aimed at optimizing louvered fin geometries tend to be costly and time-consuming because of a considerable number of geometrical parameters involved (among others, louver angle and length, as well as fin length, pitch, and thickness) and complex relationships between these parameters and device's performance figures [10]. For the sake of accurate evaluation as well as shortening the development cycle, the design processes are nowadays more and more relying on computer models rather than on physical prototypes [11,12]. The fundamental design tools involve computational fluid dynamics (CFD) simulations [13] utilizing numerical solutions of the fluid governing equations. CFD models offer an accurate evaluation of the structure at hand; however, their downside is high computational cost. In particular, CFD-driven design optimization may be impractical when using conventional techniques such as gradient search with numerical derivatives. One of the methods to accelerate the optimization process is by using fewer evaluations or to exploit a simplified computational model. Typically, function-approximation surrogate models are used, i.e., constructed by means of the design of experiments and simulation data acquisition and fitting [14]. Function-approximation models are versatile, however, they normally require a substantial amount of data samples to ensure good accuracy. Typically, these models are set up in the entire design space [15]. More efficient methods involve surrogate-based optimization with physical surrogates, e.g., suitably corrected lower-fidelity simulation models [16]. Utilization of physics-based surrogates is not widespread in the context of CFD modeling of compact heat exchangers of complex geometries.

Enhancement of convective heat transfer can be realized by means of reducing the thickness of a thermal boundary layer, increasing the distur-

bance in a fluid, and increasing the velocity gradient at the solid wall.

The foregoing literature review indicates that in all available studies, the main emphasis was put on studying the effects of geometry parameter adjustment on the average air side heat transfer and the pressure drop characteristics of heat exchangers [7,17–19].

In this study, a two-dimensional numerical simulation of the air-side heat transfer and flow characteristics of the louvered fin-and-plate heat exchanger has been presented. Our investigations are carried out by varying both the louver pitch and the angle while modifying its geometry by changing the number of louvers in a bank. The transferred heat and the pressure drops have been investigated. The heat transfer performance for various fin geometries and dimensions has been obtained. The effects of pitch, angle, and louvers number on temperature and pressure drop have been studied at for the angle range from 10° to 70°. The predictions of the pressure and air temperature drop have been compared with available experimental data.

2 Computational model

Louvered plate fins are frequently used on the air side of air conditioning evaporators and other heat exchangers to enhance the overall heat transfer rate. Figure 1 shows the overview of a multi-louvered plate heat exchanger. The present study focuses on CFD parametric study of louvered fins plate heat exchanger for varying geometry. The following parameters are considered: louver angle, louver pitch and the number of louvers in the bank. Table 1 presents a list of all geometrical parameters used in calculations. The air flow direction is x-direction, the fin spanwise direction is y-direction and fin thickness direction is z-direction. Figure 2 shows the computational domain of the louvered fin. The computation domain was extended two times beyond the fin pitch of the original heat transfer zone for the entrance section to ensure the inlet uniformity, and at the exit, the domain was extended five times fin pitch in order to make sure that the exit flow boundary has no flow recirculation. Similar conditions were considered by many researchers [17,18], and have proven to predict experimental data within acceptable accuracy. Also, numerical simulations in 3D computational domain were carried out [7,19]. The grid system for the computation domain generated by commercial software ANSYS Gambit [20] is shown in Fig. 3, where the upstream and downstream parts of the computation

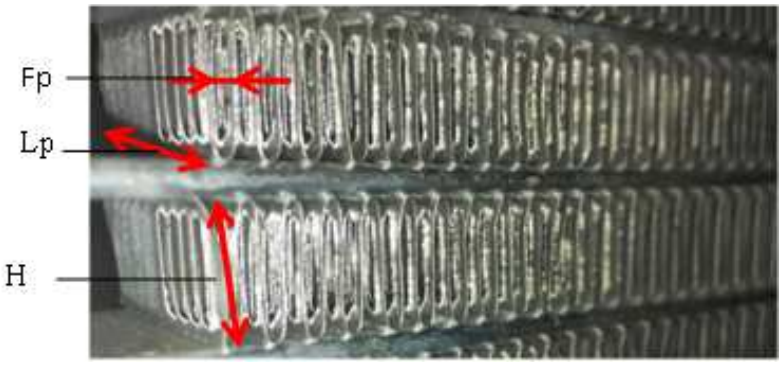

Figure 1: The overview of the multilouvered fin plate heat exchanger.

Table 1: Geometrical and working parameters of the tested evaporator of the air source heat pump.

Parameter	Value and unit
Fin thickness, F_t	0.1 mm
Number of louvers in bank	6–8
Fin pitch, F_p	2 mm
Louver pitch, L_p	0.9–1.4 mm
Louver angle	10–70
Fin length, L	36.6 mm
Louver width, H	6.53 mm
Inlet air temperature	290 K
Fin temperature	280 K
Inlet air velocity	2–8 m/s

domain are not presented in order to save the space. A grid convergence check indicated that the solution for the selected geometry consisting of approximately 400 000 elements results in about 2% offset compared to 1.6 million element grid.

The governing equations, for the forced steady, laminar, incompressible fluid flow and heat transfer in the physical space are as follows [20]: continuity equation

$$\frac{\partial}{\partial x_i}\left(\rho u_i\right) = 0 \,, \tag{1}$$

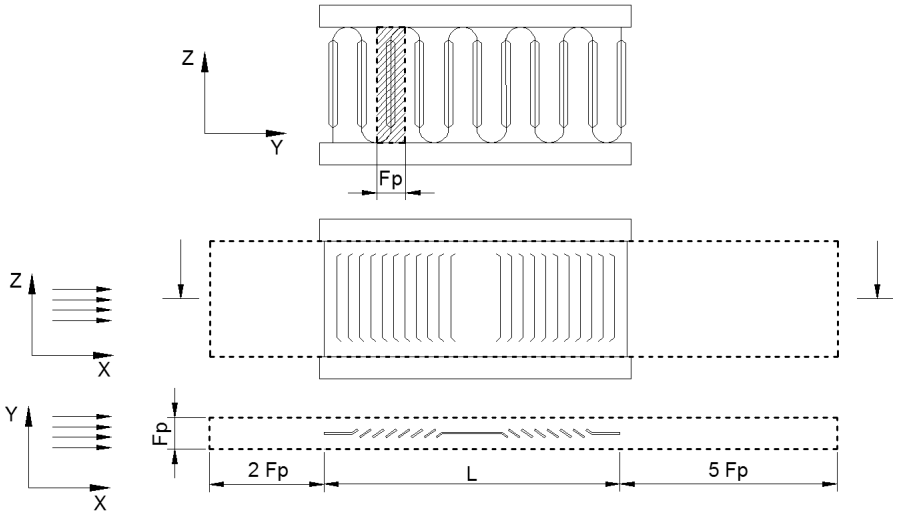

Figure 2: Schematic of louvered fins-plate heat exchanger computational domain.

(a) (b)

Figure 3: Two dimensional grid representation: (a) overview, and (b) close-up.

momentum equation

$$\frac{\partial}{\partial x_i}\left(\rho u_i u_k\right) = \frac{\partial}{\partial x_i}\left(\mu \frac{\partial u_k}{\partial x_i}\right) - \frac{\partial p}{\partial x_k}\,, \tag{2}$$

energy equation

$$\frac{\partial}{\partial x_i}\left(\rho u_i T\right) = \frac{\partial}{\partial x_i}\left(\frac{k}{c_p}\frac{\partial T}{\partial x_i}\right)\,. \tag{3}$$

The fluid is assumed to be incompressible with constant properties and the flow is laminar in a steady state condition. The temperature of the

fin surface is lower than that of the inlet air. The problem is simplified to a two-dimensional geometry, thus regarding velocity in z-direction (as depicted in Fig. 2). The boundary conditions are described for the three regions and are as follows

a) In the upstream extended region (domain inlet):
at the inlet boundary: $u = u_{in} = \text{const}$, $T = T_{in} = \text{const}$, $v = w = 0$;
at the upper and lower boundaries: $\frac{\partial u}{\partial y} = \frac{\partial w}{\partial y} = 0$, $v = 0$, $\frac{\partial T}{\partial y} = 0$.

b) In the downstream extended region (domain outlet):
at the upper and lower boundaries: $\frac{\partial u}{\partial y} = \frac{\partial w}{\partial y} = 0$, $v = 0$, $\frac{\partial T}{\partial y} = 0$;
at the outlet boundary: $\frac{\partial u}{\partial x} = \frac{\partial v}{\partial x} = \frac{\partial w}{\partial x} = 0$, $\frac{\partial T}{\partial x} = 0$.

c) In the fin region:
velocity on fin surface: $u = v = w = 0$;
temperature on fin surface: $T = \text{const}$.

All the procedures, including solver interfaces, modeling algorithms, and design specification scaling techniques were created as stand-alone routines implemented in Matlab environment [21]. Equations presented in previous sections are discretized using the finite volume technique. The equations are integrated over the individual computational cells, for steady state conditions over a domain. First-order upwind spatial discretization scheme is used both in the case of momentum and energy equations. For the pressure field calculations in steady state, the SIMPLE (semi-implicit method for pressure linkede equations) i, k – algorithm [20] is used in the commercial ANSYS FLUENT CFD [20] software toll, which uses a control-volume-based technique to convert the governing equations to algebraic equations that can be solved numerically. This involves subdividing the region in which the flow is to be solved into individual cells or control the volumes so that the equations can be integrated numerically.

3 Numerical results

In order to validate the numerical simulation reliability, geometrical dimensions described by Dong *et al.* [10] have been implemented in the computational domain and the results of numerical calculations were compared with original experimental data. Figure 4 compares experimental data with the simulation results. Calculations were made for varying inlet air velocity as indicated in Tab. 1. Steady state laminar incompressible

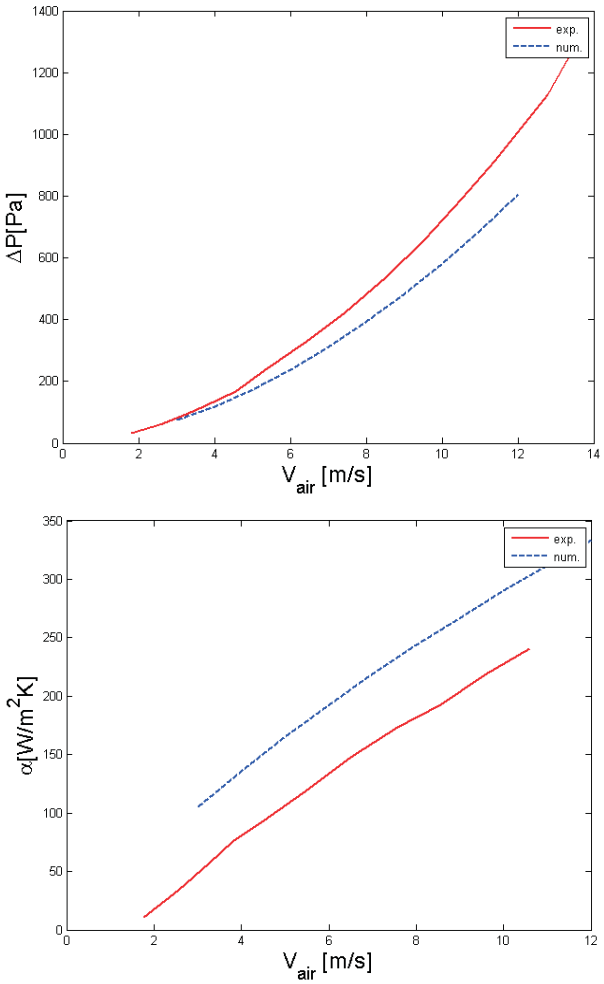

Figure 4: Experimental data by Dong *et al.* [10], compared to corresponding numerical data.

flow simulations exhibit sufficient consistency with the experimental data. The discrepancy between measurements and simulations in terms of the heat transfer is clearly visible as a constant shift between the data sets in the entire range of air velocity. This is because calculations are simplified and assume constant fin temperature, and do not include fin height which is assumed constant. The deviation between the pressure drop is much smaller with both data sets showing similar trends as a function of the air

velocity. Overall, the correlation between experimental and simulation data is sufficient to justify the utilization of computational model in searching for the optimal fin geometry.

Selected numerical results are shown in Figs. 5 through 7. The contours of the pressure, temperature and velocity are presented for the inlet air velocity of 3 m/s. It can be observed that at the low air velocity, most of the air flows through the gap between the fins rather than through the louvers. This can be attributed to the high flow resistance presented by the louvers. Since the air has less kinetic energy, most of it passes through the path of least resistance, i.e., through the fin gaps. The air temperature reaches the fin temperature in the first row of the louvers. Consequently, the heat transfer performance of the fin is poor (see Fig.7). The second half of the fin only accounts for the pressure loss without any significant heat transfer. At higher velocity, the thermal layers around the louvers are thinner and the flow is more aligned with the louvers. In this case, the temperature of the air does not decrease as fast as along the flow direction, and a significant temperature difference is maintained between air and the fin. Hence, the heat transfer rate is increased with the increased air velocity.

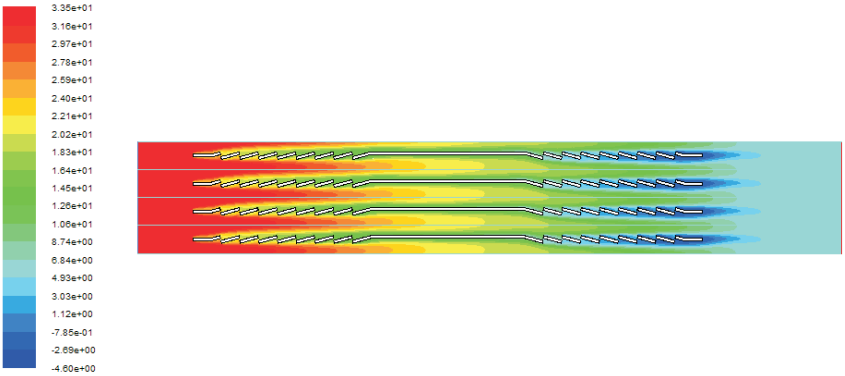

Figure 5: Contours of total pressure in pascals for $v_{air} = 3$ m/s.

Figure 5 show the total pressure distribution across the louvered fin. It can be observed that the low-pressure zone is formed near the louvers due to formation of the boundary layer. The air flowing through the louvers impinges on the flat plate and it is turned. This flow diversion results in a high-pressure zone in the middle plane, and this effect is more pronounced for increasing air velocity. These conjectures are in correspondence with obtained velocity profiles shown in Figs. 6.

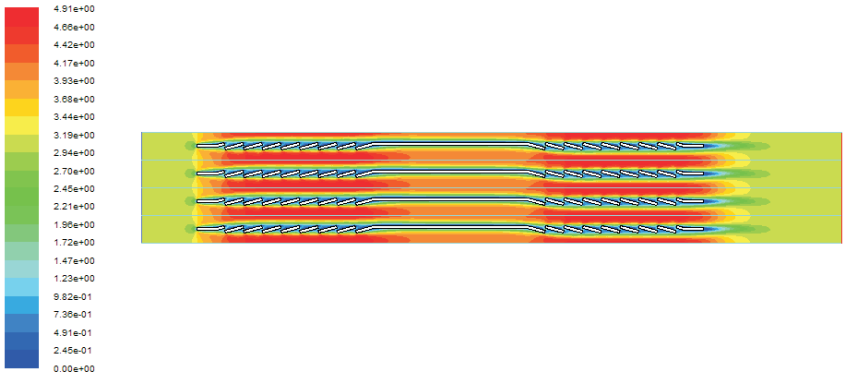

Figure 6: Contours of velocity magnitude in m/s for $v_{air} = 3$ m/s.

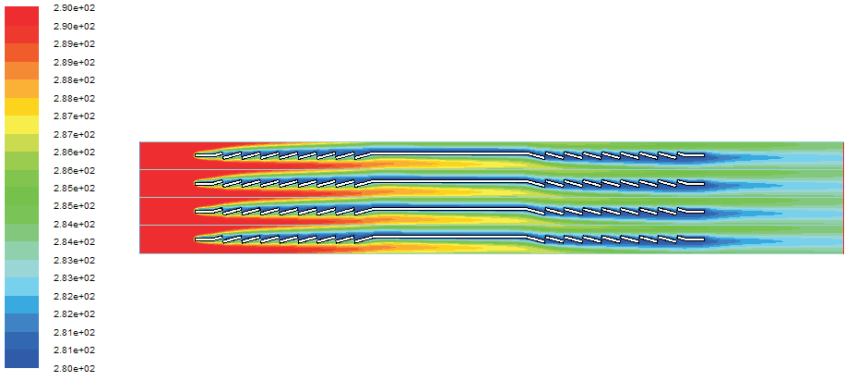

Figure 7: Contours of total temperature in kelvins for $v_{air} = 3$ m/s.

The heat transfer from the ambient air in the gap between the two fins to the refrigerant inside the tube, and the total pressure drop values of air across the heat exchanger were calculated numerically for each geometry model. With assumed constant air properties, i.e., density and specific heat, transferred heat is proportional to the volumetric flow rate and temperature drop. The results are presented in the form of obtained air temperature drop, calculated as a difference between the average temperatures on the inlet and the outlet boundary, for constant air flow rate:

$$\triangle T = \overline{T}_{in} - \overline{T}_{out} \ , \tag{4}$$

where overbar stand for area-averaged value. The pressure drop of air

passing through the fins is also taken into consideration:

$$\triangle P = \overline{P}_{in} - \overline{P}_{out} \ . \tag{5}$$

Figures 8 and 9 show the simulated heat transfer and pressure drop characteristics, presented in terms of the obtained temperature and pressure drops calculated from Eqs. (10) and (11). The values have been calculated using geometry parameters such as the louver pitch, Lp, louver angle, α, and the number of louver blades from configurations presented in Tab. 1 and Fig. 2. The calculated temperature and the pressure drop values for the varying velocities were also provided to compare with variable louver pitch and angles. The total heat transfer rate was normalized in form of ΔT to ensure fair comparison in all cases. It can be observed from the results gathered in plots that the best heat transfer per segment was obtained for the louver angle of 70° and the louver pitch equal to 1.35 mm. The maximum normalized heat transfer enhancement was 14%. The maximum enhancement of the heat transfer is associated with pressure drop per segment that is 10 times higher than for the reference case.

Figure 8 shows the effect of the louver angle and pitch on the pressure drop. It can be observed that the pressure drop increases with the louver angle and reaches its maximum value at 70°. Furthermore, it decreases with the decreased louver pitch for all cases. The pressure drop increases rapidly with the louver angle higher than 40°. This is because at higher velocities – which corresponds to higher Reynolds numbers – the flow is aligned with the louver angle. Larger louver angles increase the flow blockage and enforce more flow through the louver blades. Figure 9 shows the effects of the same geometry parameters on the simulated temperature drop. The rapid drop can be observed in all cases for louver angles below 20°. This drop is more rapid in the case of larger louver pitch values. The relatively flat response can be observed for louver angles between 20° and 40°. The effect of louver pitch on the obtained ΔT is more visible in case of higher louver angles, where it attains its maximum value for $\alpha = 70°$ and $Lp = 1.3$–1.4 mm which corresponds to maximum ΔP.

A simple method of selecting the optimal geometry can be formulated as follows. The pressure drop is a function of the friction factor based on the fin surface condition and position. Thus, an engineer is frequently interested in the pressure drop needed to sustain an internal flow because this parameter determines the fan power requirements. The hydraulic pumping power, W, required to overcome the resistance to the flow associated with this pressure

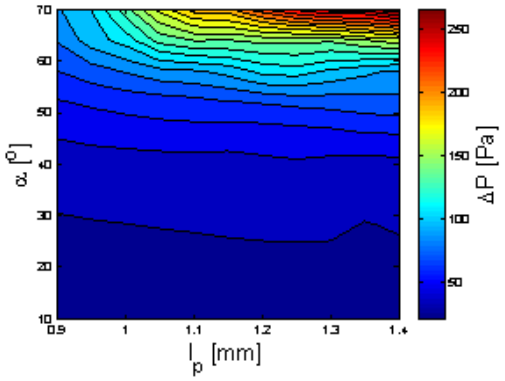

(a)

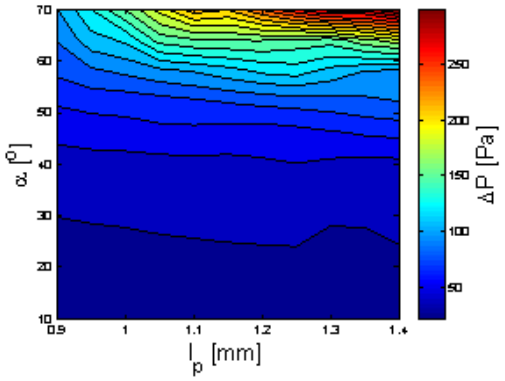

(b)

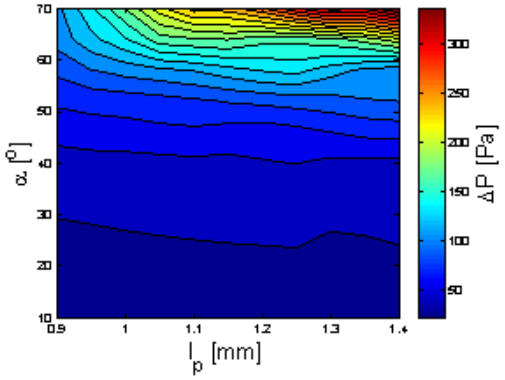

(c)

Figure 8: Numerically predicted pressure drop for air velocity $v_{air} = 3$ m/s, for (a) six, (b) seven, and (c) eight louvers.

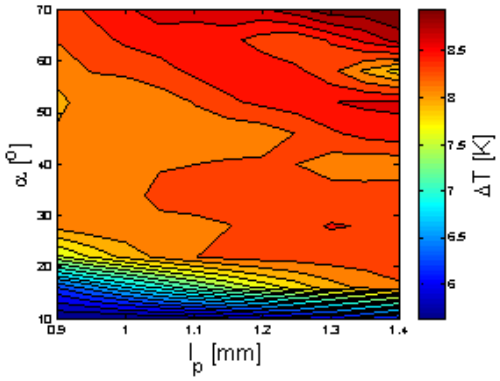

(a)

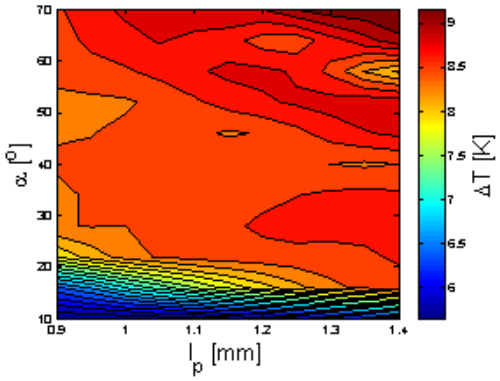

(b)

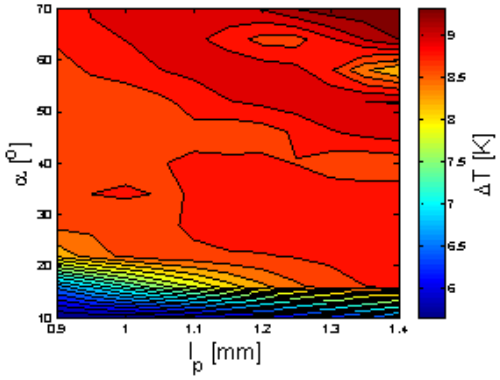

(c)

Figure 9: Numerically predicted temperature gradient for air velocity $v_{air} = 3$ m/s, for (a) six, (b) seven, and (c) eight louvers.

drop ΔP may be expressed as

$$P_h{=}\triangle P\,\dot{V}\ , \tag{6}$$

where the volumetric flow rate, $\dot{V}$, may, in turn, be expressed as $\dot{V}{=}\dot{m}/\rho$, i.e. the ratio of mass flow rate $\dot{m}$ and mass density ρ (kg/m3 for an incompressible fluid. The power required to move the fluid across the bank is often a major operating expense and is directly proportional to the pressure drop. Heat transferred from ambient air to the high pressure evaporator can be calculated as

$$\dot{Q}{=}\dot{V}\,\rho\,c_p\,\triangle T\ . \tag{7}$$

Overall thermal performance of the heat exchanger can be expressed as a ratio of the pumping power to the transferred heat, as dimensionless index

$$\eta = \frac{\dot{Q}}{P_h} = \frac{\rho\,c_p\,\triangle T}{\triangle P}\ . \tag{8}$$

Figure 10 shows the effect of the geometry parameters on the performance calculated using (8). Rapid performance drop can be observed in all cases for louver angles larger than 40°. Furthermore, a maximum performance region can be identified, for all considered cases, for the louver angle ranging from 16 to 20°. This region is shifted towards the lower louver pitch for the increased number of louver blades. As previously described, the simulations were repeated for air velocities from 3 to 8 m/s. The maximum performance region is shifted towards the higher louver pitch values for the decreased inlet air velocity. The maximum performance for cases from the whole computational domain can be compared to identify the influence of changing the number of the louver blades. The maximum performance in all cases was obtained for the louver angle $\alpha = 16°$. Figure 11 shows a single maximum performance point as a function of air velocity (for variable α and Lp). It can be observed that the performance is higher for lower air velocities. Also, a slight increase of performance can be observed between the compared cases.

As mentioned earlier, the maximum performance was obtained for the louver angle $\alpha = 16°$. Therefore, its influence is not depicted. In all cases, the louver pitch length smaller than $Lp = 1.2$ mm resulted in degraded performance compared to the optimal value. As indicated in Fig. 12, the maximum performance is obtained for different louver blade numbers and pitch. For higher inlet air velocities, the maximum performance is obtained for a smaller length of the louver pitch.

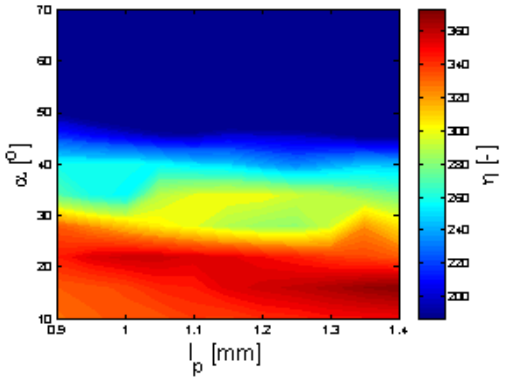

(a)

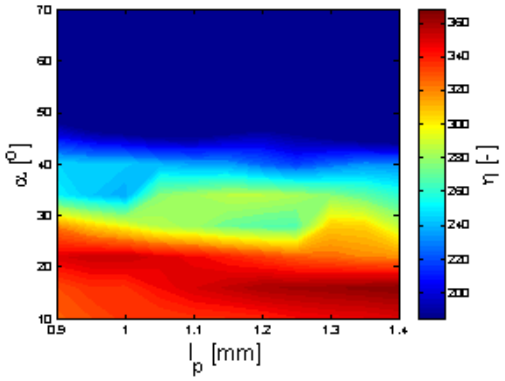

(b)

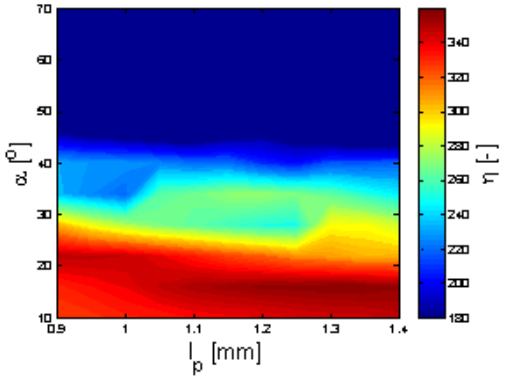

(c)

Figure 10: Numerically predicted temperature gradient for air velocity $v_{air} = 3$ m/s, for (a) six, (b) seven, and (c) eight louvers.

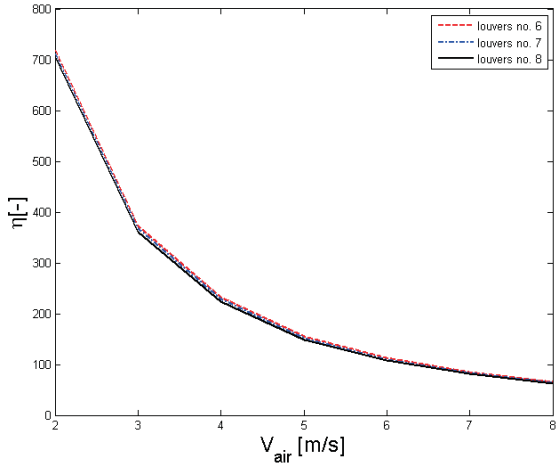

Figure 11: Maximum performance as a function of frontal air velocity for selected geometries.

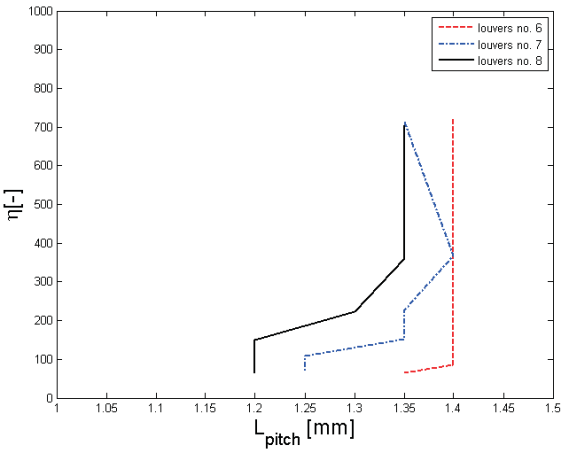

Figure 12: Maximum performance as a function of louver pitch for selected geometries.

4 Conclusion

Numerical simulations of compact louvered fin heat exchangers have been performed in order to determine heat transfer and pressure drop characteristics. A total of 363 different configurations has been studied. For the sake of validation of the computational model, the simulation results have been

compared with experimental data. The computed heat transfer coefficients and pressure drops are found to be in good agreement with the experiment within the considered flow range. A simple procedure for identifying the optimal geometry has been presented. A parametric variation of the geometry provides a map to find the desired configuration for which the heat transfer to the pressure drop ratio attains its maximum. Furthermore, for each louver blade number and air inlet velocity, a region with a local maximum of performance can be found. Among all considered geometry parameters, the louver angle of 16° yields the maximum performance for all considered combinations of the flow rate and the louver pitch. The future work will be focused on the development of numerical optimization techniques for finding the optimum heat exchanges geometry as well as including a heat exchanger size cost factor in the optimization process.

Acknowledgements Calculations were carried out at the Academic Computer Centre TASK in Gdańsk.

Received 16 June 2016

References

[1] Cengel Y.A., Boles M.A.: *Thermodynamics: An Engineering Approach*, McGraw-Hill, 2015.

[2] Kandlikar S.G.: *Two-phase flow patterns, pressure drop, and heat transfer during boiling in minichannel flow passages of compact evaporators*. Heat Trans. Eng. **23**(2002), 5–23.

[3] Taler D.: *Mathematical modeling and control of plate fin and tube heat exchangers*. Energy Convers. Manag. **96**(2015), 452–462 (DOI:10.1016/j.enconman.2015.03.015).

[4] Hepbasli A., Kalinci Y.: *A review of heat pump water heating systems*. Renew. Sustain. Energy Rev. **13**(2009), 1211–1229 (DOI:10.1016/j.rser.2008.08.002).

[5] Mikielewicz D., Muszyński T., Mikielewicz J.: *Model of heat transfer in the stagnation point of rapidly evaporating microjet*. Arch. Thermodyn. **33**(2013), 1, 139–152.

[6] Mikielewicz D., Jakubowska B.: *Prediction of flow boiling heat transfer coefficient for carbon dioxide in minichannels and conventional channels*. Arch. Thermodyn. **37**(2016), 2, 89–106.

[7] Gunnasegaran P., Shuaib N.H., Abdul Jalal M.F., Gunnasegaran P., Shuaib N.H., Abdul Jalal M.F.: *The effect of geometrical parameters on heat transfer characteristics of compact heat exchanger with louvered fins*. ISRN Thermodyn. 2012 (2012) 1–10 (DOI:10.5402/2012/832708).

[8] Wang C.-C. Lee, W.-S., Sheu W.-J.: *A comparative study of compact enhanced fin-and-tube heat exchangers*. Int. J. Heat Mass Transf. **44**(2001), 3565–3573. doi:10.1016/S0017-9310(01)00011-4.

[9] Zhang X., Tafti D.: *Flow efficiency in multi-louvered fins*. Int. J. Heat Mass Transf. **46**(2003), 1737–1750 (DOI:10.1016/S0017-9310(02)00482-9).

[10] Dong J., Chen J., Chen Z., Zhang W., Zhou Y.: *Heat transfer and pressure drop correlations for the multi-louvered fin compact heat exchangers*. Energy Convers. Manag. **48**(2007), 1506–1515 (DOI:10.1016/j.enconman.2006.11.023).

[11] Xia Y., Zhong Y., Hrnjak P.S., Jacobi A.M.: *Frost, defrost, and refrost and its impact on the air-side thermal-hydraulic performance of louvered-fin, flat-tube heat exchangers*. Int. J. Refrig. **29**(2006), 1066–1079 (DOI:10.1016/j.ijrefrig.2006.03.005).

[12] Kim S.Y., Paek J.W., Kang B.H.: *Flow and heat transfer correlations for porous fin in a plate-fin heat exchanger*. J. Heat Transfer. **122**(2000), 572 (DOI:10.1115/1.1287170).

[13] Ameel B., Degroote J., Huisseune H., De Jaeger P., Vierendeels J. et al.: *Numerical optimization of louvered fin heat exchanger with variable louver angles*. J. Phys. Conf. Ser. **395**(2012), 12054 (DOI:10.1088/1742-6596/395/1/012054).

[14] Leifsson L., Koziel S.: *Aerodynamic shape optimization by variable-fidelity computational fluid dynamics models: A review of recent progress*. J. Comput. Sci. **10**(2015), 45–54 (DOI:10.1016/j.jocs.2015.01.003).

[15] Koziel S., Ciaurri D.E., Leifsson L.: *Surrogate-based methods*. Stud. Comput. Intell. **356**(2011), 33–59 (DOI:10.1007/978-3-642-20859-1_3).

[16] Koziel S., Ogurtsov S., Leifsson L.: *Knowledge-based response correction and adaptive design specifications for microwave design optimization*. In: Procedia Comput. Sci., 2012: 764–773 (DOI:10.1016/j.procs.2012.04.082).

[17] Hsieh C.T., Jang J.Y.: *3-D thermal-hydraulic analysis for louver fin heat exchangers with variable louver angle*. Appl. Therm. Eng. **26**(2006), 1629–1639 (DOI:10.1016/j.applthermaleng.2005.11.019).

[18] Malapure V.P., Mitra S.K., Bhattacharya A.: *Numerical investigation of fluid flow and heat transfer over louvered fins in compact heat exchanger*. Int. J. Therm. Sci. **46**(2007), 199–211 (DOI:10.1016/j.ijthermalsci.2006.04.010).

[19] Ameel B., Degroote J., Huisseune H., De Jaeger P., Vierendeels J., De Paepe M.: *Numerical optimization of louvered fin heat exchanger with variable louver angles*. J. Phys. Conf. Ser. **395**(2012), 12054 (DOI:10.1088/1742-6596/395/1/012054).

[20] *Fluent*. ANSYS Fluent 12.0 user's guide, Ansys Inc. 15317 (2009) 1–2498 (DOI:10.1016/0140-3664(87)90311-2).

[21] *Matlab documentation*. Matlab. (2012) R2012b (DOI:10.1201/9781420034950).